



GEOMETRIC ANALYSIS OF TIBIOFEMORAL KNEE JOINT: TOWARDS COMPUTER AIDED TREATMENT (CAT) PLANNING

Humera Tariq^{a*}, Syed Faraz^b, Asia Samreen^c, and Usman Amjad^a

^a Department of Computer Science, University of Karachi, Karachi, PAKISTAN

^b Center for Intelligent Signal and Imaging Research (CISIR), Universiti Teknologi PETRONAS, Tronoh, Perak, MALAYSIA

^c Department of Computer Science, Bahria University, Karachi, PAKISTAN

ARTICLE INFO

Article history:

Received 07 January 2019
Received in revised form 05
March 2019
Accepted 12 March 2019
Available online
14 March 2019

Keywords:

Bone Modeling; Joint
Modeling; Varus;
Valgus; Joint space
width; Anatomic axis
Angle; Condylar angle.

ABSTRACT

Two Dimensional Geometric Analysis and Modeling become increasingly important in computer-aided treatment (CAT) planning, non-invasive surgical processes, computer-aided diagnostic (CAD), computer aided modeling (CAM) and disease progression. The purpose of this article is to present a computer-aided geometrical analysis of tibiofemoral joint from knee radiographs from a computing perspective. Lateral and Medial Joint Space Width (JSW), anatomical axis angle (AAA), Femorotibial angle (FTA), Condylar Plateau Angle (CPA), Condylar Angle (CA) and Tibial Plateau Angle (TPA) has been Quantified with novel linear algebra abstractions with an intention to use in 3D Joint Modeling and Animation. Edge pixel Detection, curve modeling, and linear regression have been expended as key methods to estimate anatomical axes and respective angles. Implementation details of methodology have been presented in the form of code listing. Quantification of aforementioned knee parameters has been successfully quantified with 85% accuracy over an originally acquired patient dataset in DICOM (Digital Imaging and COmmunications in Medicine) Format.

© 2019 INT TRANS J ENG MANAG SCI TECH.

1. INTRODUCTION

Bone and Joint Modeling in 2D and 3D become increasingly important with recent advancement in Medical Sciences (Imhauser and Schafer, 2019; Burluson and Dipaola, 2019) for e.g. Orthopedic surgeons need specialized software to decide about bone and joint measurements for treatment and replacement purpose (Belvedere et al., 2018). This new dimension of science and technology lies at the intersection of interesting Engineering and computer science subjects namely: (1) Digital Image Processing (2) Computer Graphics (3) Kinetics and kinematics (Ghorbel et al., 2018; Alnouri et al., 2015; Gonzalez and Woods, 2008; Hill, 2007; Aguado, & Alberto, 2018). This particular paper is written for early-stage computer scientists, engineers, and researchers to build understanding about

utilizing higher level mathematics and computing for the purpose of building CAD/CAT/CAM software. Figure 1 shows lines and angles to be extracted from human knee radiograph. In Figure 1, Line No. 1 is drawn to visualize femoral anatomic axis. Line No. 2, 3 and 4 represents tibial anatomic axis, Condylar line and Tibial Plateau line respectively (Harvey et. al., 2008). Associated with four lines, there also lies four angles 'a', 'b', 'c', and 'd' which represents anatomic axis angle (AAA), Femoral condylar angle(FCA), tibial plateau angle (TPA) and Condylar plateau angle (CPA) respectively. This work is an extension of previously done edge pixel detection on Knee radiographs [10].

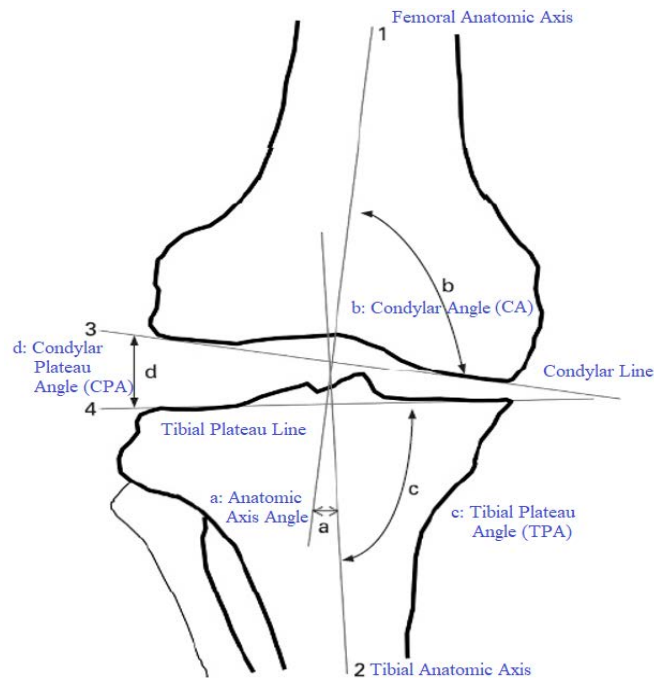


Figure 1: Lines and Angles to be extracted from the Knee (after Harvey et. al., 2008; Harvey and Hundter, 2007).

This paper is organized as follows: Section 2 discusses data acquisition and data preparation. Section 3 and Section 4 revives the theory of drawing lines and curves from edge pixels so that novice programmers and technologists grasp the mathematics and logic that are working behind commercial software which usually acquires point data from spreadsheets (Vitković et al., 2018). Section 5 contains qualitative experimental results and discussion which follows quantification in the same section. Finally, conclusion and future work are presented in Section 6.

2. PRELIMINARIES

Bone and Joint modelings start with acquiring point data which is simply a list of (x,y) pairs of coordinates. These coordinates are basically detected edge pixel from appropriate imaging modality for e.g. this work chooses DICOM images of Knee. All the Processing is done on MATLAB® due to its simplicity and built-in image processing library routines. The very first step is to write code for loading DICOM images, remove patient information and to organize them as per processing criteria for e.g. discriminate them as Male (M) and Female (F) patients as shown in Figure 2.

The first step is to prepare data for processing by automation of four preliminary steps: (1) Isolate Knee Images (2) Renaming (3) Cropping (4) Resizing. After Organizing data separately into two folders, the next step is to determine whether the current DICOM image contains the right knee or

```

clearvars;
close all;
workspace;

% Define some top-level folder.
start_path = cd
topLevelFolder = uigetdir(start_path)

datasets=dicom_folder_info(topLevelFolder,true);
[m n] = size(datasets)
for i = 1:n
    if(strcmp(datasets(i).SeriesDescription,'Knee AP'))
        datasets(i).SeriesDescription;
        info = datasets(i).DicomInfo;
        pName = info.PatientName;
        pName = char(struct2cell(pName(1:end)));
        fileName = char(strcat(pName,{' .dcm'}));
        I = dicomread(char(datasets(i).FileNames));
        dicomwrite(I, fileName,info, 'CreateMode', 'copy');
        age = char(info.PatientAge);
        age = age(1:end-1);
        d = sscanf(age,'%d')
        if(strcmp(info.PatientSex,'M'))
            movefile(fileName,strcat('Male/',fileName));
        else
            movefile(fileName,strcat('Female/',fileName));
        end
    end
end
end

```

Figure 2: Code Listing I- DICOM loader and Organizer.

left knee or both within single image space. If it contains both knees, then it needs to split into left and right knee through cropping. Cropping is comparatively a simple operation which involves extracting a pre-select rectangle portion from image space as shown in Figure 3. The images have been acquired in an entirely raw format from Esa Lab, Karachi, Pakistan for research purpose. The raw data needs specialized preprocessing for e.g. Figure 4 shows collect data from Esa lab. It contains per day scan of all types of scan for e.g. chest, knee, arm, foot in a multi-level folder of size 7GB on disk. Different libraries use different origin for cropping and spatial operation. The most frequent origin is considered right top corner instead of the bottom left corner of the whole image. With respect to the right top corner, the left half rectangle comprises of (right, top, width/2, height) while right half rectangle becomes (width/2, 0, width/2, height), see Figure 4. The third basic operation is resizing. The size property of DICOM image is not exposed or read directly, instead dedicated lines of code has been written to capture properties of DICOM in an 'info' series data structure as shown in Figure 4. DICOM are high-resolution images for e.g 3480 X 2125 and thus need resizing to 128 x 128 keep processing time optimal and uniform across all images, Figure 5.

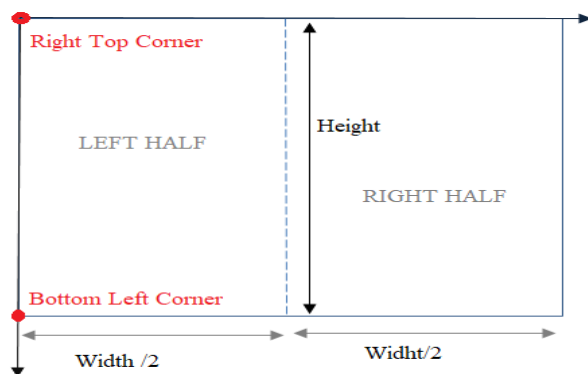


Figure 3: Cropping DICOM into Two Halves.

Multi-Level Raw DICOM Folder Structure	Size:	6.59 GB (7,082,263,150 bytes)
	Size on disk:	6.59 GB (7,083,266,048 bytes)
	Contains:	627 Files, 1,011 Folders

- 1.3.51.0.7.17492439.61168.65355.36550.6881.54692.63016
- 1.3.51.0.7.103727238.34774.44355.33917.6396.8369.29141
- 1.3.51.0.7.104123004.27639.2122.39634.9412.13638.31128
- 1.3.51.0.7.104839244.61344.33091.45006.33894.54245.33308

- 1.3.51.0.7.1315079248.53184.35905.37950.8535.42500.52856
- 1.3.51.0.7.1318301168.52160.20296.35984.45776.2198.25115
- 1.3.51.0.7.2002021459.27511.65.34164.36869.64976.25012
- 1.3.51.0.7.12336110598.29548.25678.38196.3020.15777.4996

1.3.51.0.7.3247199892.45328.4683.41560.23304.41132.62939.dcm

Figure 4: DICOM File Structure.

```

im = dicomread([filepath filelist{ind}]);
size(im);
info = dicominfo([filepath filelist{ind}]);
im=imresize(im,[256 256],'bicubic');

```

Figure 5: Code Listing II- Image Resizing.

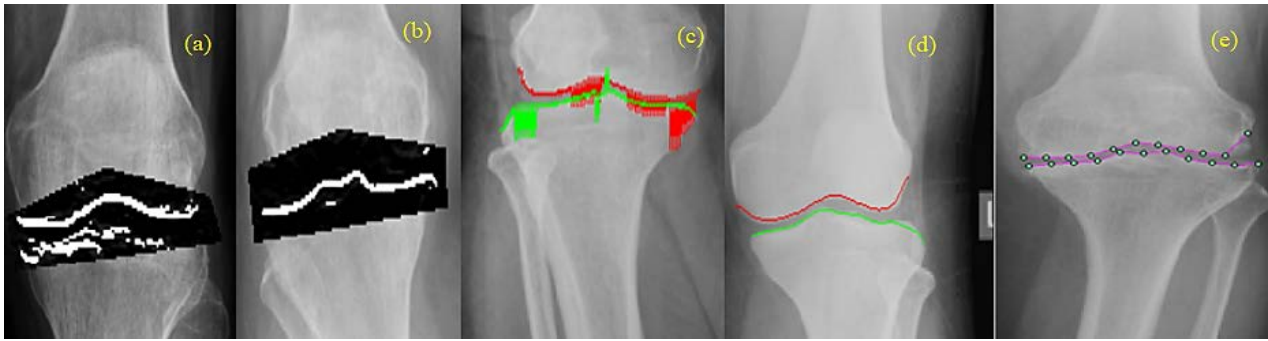


Figure 6: Code Listing II- Image Resizing

3. LITERATURE REVIEW

As we told in Section I that current work is an extension of existing work (Tariq, and Burney, 2012). Previous work covers pixel edge detection and contour formation of femoral and tibial condyle as shown in Figure 6. The Edge pixel detection process is done twice to detect upper and lower condyle pixels respectively as showing in Figure 6 (a) and Figure 6 (b). Special care is taken while selecting ROI for lower condyle otherwise noise increases afterward. Multiplying (dot multiply in MATLAB) this mask with the original image results in a new image with all the undesired (masked) parts of the image set to black. This masked image is of type single. The original image is of type uint8; Mask is of type logical; Multiplication with original image yields single (just like float takes 4 bytes, value b/w 0 &1) as shown in Figure 7. Two new images J1 and J2 have been created by applying Prewitt edge detector and its reflected counterpart as follows:

```
J1 = roifilt2(h1 ,im,inMaskImage);
J2 = roifilt2(h2 ,im,inMaskImage);
```

Figure 6 (a) and Figure 6 (b) are actually J1 and J2. Conditions have been designed to modify J1 and J2 So that they only contain condylar pixels and rest of the false detection will be eliminated. The very first condition demands for restoring original pixel values outside the mask area while the second condition requires setting the value of the pixel to white if it is true candidate condylar edge pixel, See Figure 7. The reader easily observes the appearance of false detections by edge detectors which need special attention for excluding them from the candidate pixel list. Masking is an intelligent idea to restrict processing to particular pixels to save computation over the whole image of size $N \times N$. Function roipoly is used to get the desired portion of the image from the user through mouse interaction at runtime as shown in Figure 8, Code Listing III.

```
if ( i < min(X) || i > max(X) && j > min(Y) || j < max(Y) )
    J1(i,j) = round(J1(i,j) *0.95) ;
    J2(i,j) = round(J2(i,j) *0.95) ;

[r c] = find(inMaskImage > 0);
for i = 1 : length(r)
for j =1 :length(c)
    if (inMaskImage(r(i),c(j)) > 0 && J1(r(i),c(j)) > 40)
        J1(r(i),c(j)) = 255;
    end
end
```

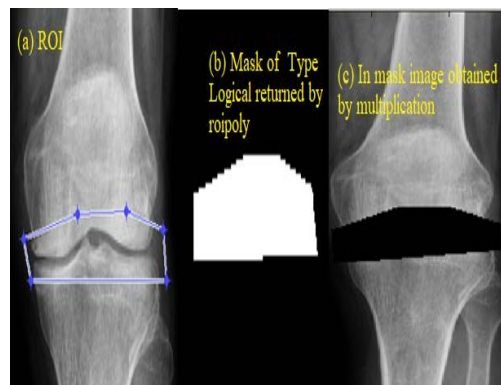


Figure 7: (a) ROI Selection (b) Logical Mask (c) In-Mask Image.

```

[BW X Y] = roipoly();
if (length(X) < 6)
message = sprintf('Wrong input,Select ROI
again');
uiwait(msgbox(message));
axes(hAxes(ind));
[BW X Y] = roipoly(im);
end

line(X, Y, 'Parent',hAxes(ind), 'color','w')
ROI = [X Y];

%row vector with x1 y1 x2 y2
ROI_array = reshape(ROI',1,[]);

for i =1: length(ROI_array)
ROI_Matrix(ind,i)= ROI_array(i);
end

ROI_Matrix;

mask = poly2mask(X,Y,size(im,1),size(im,2));

imshow(mask);
class(mask) % logical type image
inMaskImage = mask .* single(im);
imshow(inMaskImage);

```

Figure 8: Code Listing III- Masking and ROI Selection

4. SMOOTHING AND SAMPLING

Till this end, we were able to visualize edge pixels as white pixels overlay on original images namely J1 and J2 showing upper and lower condyle pixels respectively. Next step is to connect edge pixel to form a curve. Consider a few observations from sample data obtained during experimentation and analysis:

Edge-Pixels = [(80,128), (80,129), (81,128), (81,129), (81,130), (82,129), (82,130),
(82,140), (82,141), (83,129), (83,130)]

Frequency analysis of the above data yields the following results:

Frequency = [2 3 4 5 6 5 6 6 7 6]

For every x-coordinate, there exist multiple values for e.g: for x=82, there exist four possible outcomes y= 129,130,140,141 i.e. one to many correspondences exist which need to transform into one to one mapping. The rule is to pick minimum y-coordinate for the upper femoral condyle curve while picking maximum y-coordinate for lower tibial condyle curve. Comments are also shown for reader convenience and reproducibility of work. There still need another step to get smooth condylar curve namely interpolation. Below is sample data after noisy observation elimination which now shows that there are many missing values against given x-coordinate and thus need fixing this issue. Here comes spline to rescue the situation. To do so, we need to find the minimum, maximum and missing values of observations. To create equal space samples, we have used a spacing of $(\max - \min) / (\text{samplePoints})$. The drawing approach just discussed is the parametric approximation of curve $P(t) = (x(t), y(t))$ $0 \leq t \leq 1$. Sequence $\{t_i\}$ is chosen and for each $\{t_i\}$, x and y is found at that particular instance t (Hill, 2007). Code to do spline interpolation is shown in Figure 10 as Code Listing V. Figure 11 shows an important scenario when two curve overlap each other. Computation and analysis of along vertical axis is presented in Code Listing IV.

```

n11=length(UniXY11(:,1));
xplot=min(UniXY11(:,1)):(max(UniXY11(:,1))-
min(UniXY11(:,1)))/10000:max(UniXY11(:,1));

yplot=spline(UniXY11(:,1),UniXY11(:,2),xplot);

yplot = smooth(yplot,0.1);
plot(xplot,yplot,'color','r');

```

Figure 10: Code Listing of Spline Interpolation

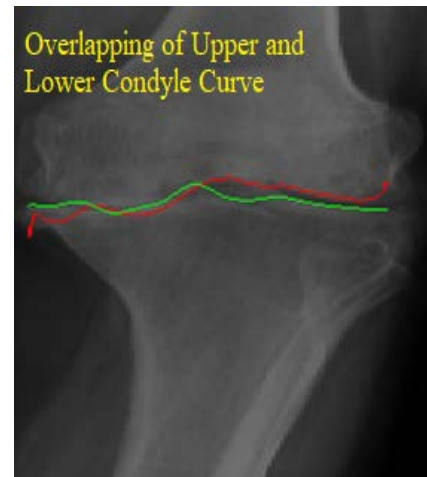


Figure 11: curve overlapping

```

for z = 1: length(Number1) % z is row no and Number1 is x value i.e.
                           %80,81,82..|...
if ( numTimesInMatrix1(z) >1) % if frequency is greater than 1 which
                               %is almost true for everyx
    count1 = numTimesInMatrix1(z); % get frequency in count1 say 4 times
    num1 = Number1(z); % get x value in num1 say 80
    id1 = find(UniXY1(:,1)==num1); % find index corresponding to multiply
    % x values say 80
    X1 = UniXY1(id1,1); % get x at that indexes
    Y1 = UniXY1(id1,2) ; % get y at that indexes
    Ymin = min(Y1); % get the miny value amongst all for upper condyle
    UniXY1(id1,1) = X1 ; % now x remains same in uppercondyle array
    UniXY1(id1,2) = Ymin;% replace all y's with min Y
end
end
for z = 1: length(Number2) % z is row no.
if ( numTimesInMatrix2(z) >1)
    count2 = numTimesInMatrix2(z);
    num2 = Number2(z);
    id2 = find(UniXY2(:,1)==num2);
    X2 = UniXY2(id2,1);
    Y2 = UniXY2(id2,2) ;
    %Ymax = max(Y1); % lower condyle
    Ymax = mean(Y2); % lower condyle
    UniXY2(id2,1) = X2 ;
    UniXY2(id2,2) = Ymax;
end
end
imshow(im);
hold on;
%plot of unique spatial coordinates of upper condyle
[UniXY11,Ix]=unique(UniXY1,'rows'); plot(UniXY11(:,1),UniXY11(:,2),'color','r');
%plot of unique spatial coordinates of lower condyle
[UniXY22,Ix2]=unique(UniXY2,'rows'); plot(UniXY22(:,1),UniXY22(:,2),'color','g');

```

Figure 9: Code Listing IV Eliminating noisy and redundant observations

5. GEOMETRIC ANALYSIS AND RESULTS

Linear regression has been in practice since long by surgeons in literature for drawing of the anatomical axis from knee radiographs (Okamoto et. al., 2014), (Goulston et. al., 2016), (Colebatch et. al., 2009), (Harvey, and Hundter, 2007). In our case, samples have been successfully generated using spline interpolation in the form of two vectors $X_{Upper} = [x_1, x_2, x_3, \dots, x_n]$ and $Y_{Upper} = [y_1, y_2, y_3, \dots, y_n]$. Similarly $X_{Lower} = [x_1, x_2, x_3, \dots, x_n]$ and $Y_{Lower} = [y_1, y_2, y_3, \dots, y_n]$.

It has been observed from Figure 1 that Condylar Line labeled as 3 and Tibial Plateau Line labeled as 4 has been passing through extreme points of the upper and lower condylar curve thus regression through curve points employ subset of both $P_{upper} = (x_{upper}, y_{upper})$ and $P_{lower} = (x_{lower}, y_{lower})$. Selection requires trimming at both ends of upper and lower point lists. Linear Regression to draw Condylar and Tibial Plateau Line is expressed as follows:

$$y_{condylar} = \beta_0 + \beta_1 X_{Upper}^{Extreme} \quad (1).$$

The notation $X_{Upper}^{Extreme}$ is used to represent selected extreme xy coordinates from Upper Point list. These points are shown in magenta color on upper condyle while with Pale yellow on lower condyle as Candidate pixels for Regression. Similarly,

$$y_{tibial\ plateau} = \alpha_0 + \alpha_1 X_{Upper}^{Extreme} \quad (2).$$

To determine midpoint as anatomical axis passes through it mean of estimated spline curve data has been used as shown in EQ (3) and Figure 13 (a):

$$P_{mid-central} = (\text{mean}(X_{lower}), \text{mean}(Y_{lower})) \quad (3)$$

Next User is asked to input two points manually on the femur and tibial bone with the help of which further mid-points has been determined. Joining femur and central midpoint results in femoral anatomical axis (FA) while joining tibial and central mid-point results in tibial axis (TA) as shown in Figure 13 (b). The line has been drawn parametrically using Equation (4):

$$P(t) = A + (B - A)t \quad 0 \leq t \leq 1 \quad (4)$$

Since both anatomical axes have drawn successfully so it is now easy to determine anatomic axis angle (AAA) or Femoral Tibial Angle (FTA) as follows:

$$\begin{aligned} \bar{v}_{FA} &= P_{mid}^{Femur} - P_{mid-central}, \text{ and} \\ \bar{v}_{TA} &= P_{mid}^{Tibia} - P_{mid-central} \\ \theta_{AAA} \text{ (degrees)} &= \cos^{-1} \left(\frac{\bar{v}_{FA} \cdot \bar{v}_{TA}}{|\bar{v}_{FA}| \cdot |\bar{v}_{TA}|} \right) * \left(\frac{180}{PI} \right) \end{aligned} \quad (5)$$

The Condylar Plateau angle (CPA) between two regression lines can be estimated similarly by finding two appropriate direction vectors and taking cosine inverse of them. First direction vector \bar{v}_{TP} is along tibial plateau regression line, shown in Magenta color on the right side in Figure 12, Figure 13 and Figure 14 respectively. The second direction vector \bar{v}_{FP} is along Femoral Plateau regression line shown in Blue in same figures. Thus CPA calculation is possible by implementing Equations (6) and (7) in a system. Same direction vector logic is used to find the Tibial Plateau angle (TPA) and condylar angle (CA).

$$\bar{v}_{FP} = P_{FP}^B - P_{FP}^A \quad (6),$$

$$\bar{v}_{TP} = P_{TP}^B - P_{TP}^A \quad (7),$$

$$\theta_{CPA} \text{ (degrees)} = \cos^{-1} \left(\frac{\bar{v}_{FP} \cdot \bar{v}_{TP}}{|\bar{v}_{FP}| \cdot |\bar{v}_{TP}|} \right) * \left(\frac{180}{PI} \right) \quad (8).$$

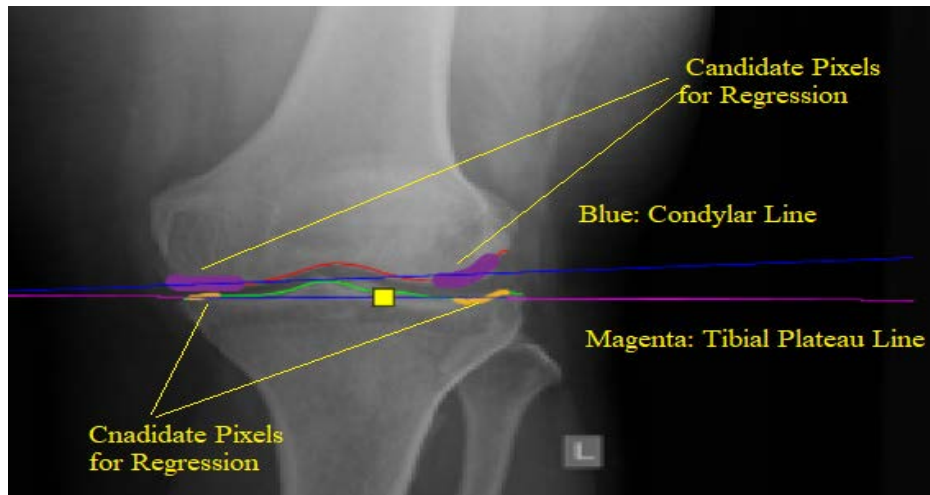


Figure 12: Candidate Pixels for Regression

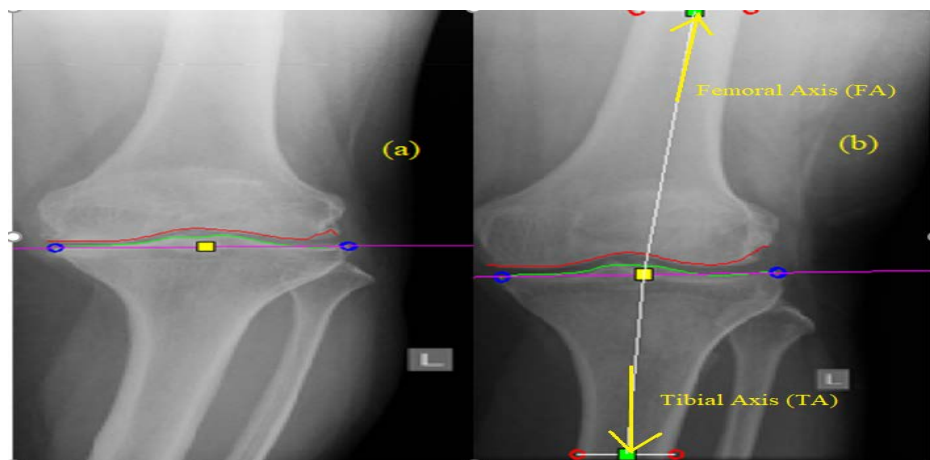


Figure 13: (a) Mid-Point (b) Femoral and Tibial Anatomic Axis.

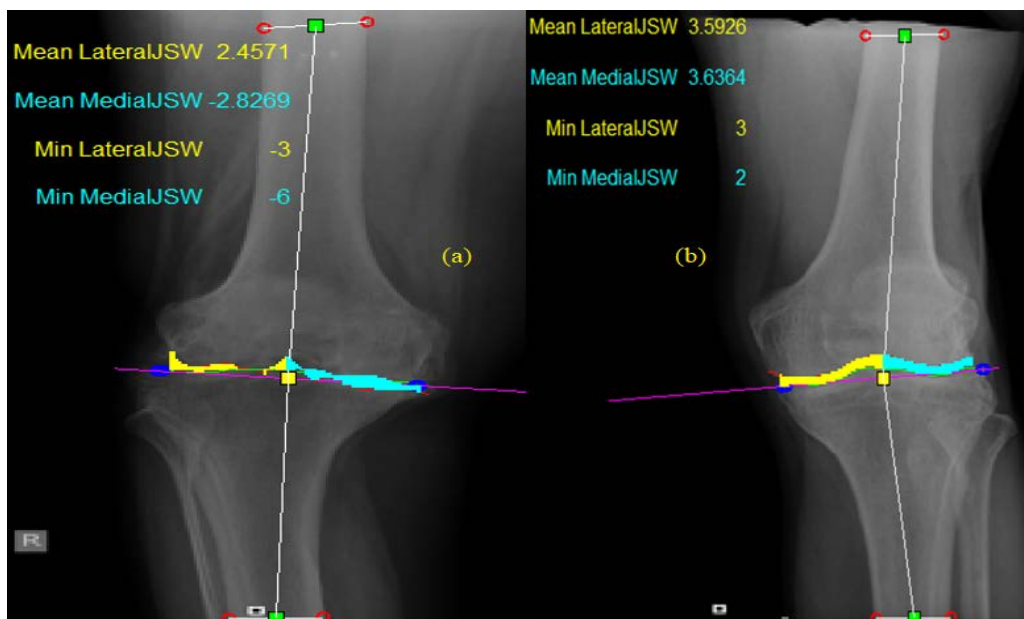


Figure 14: Joint Space Width (JSW) (a) negative JSW (b) Positive JSW

After building geometric interpretation of four angles Anatomical Axis Angles (AAA), Condylar Plateau Angle (CPA), Tibial Plateau Angle (TPA) and Condylar angle (CA), it is also possible to measure lateral and medial Joint space width between two condylar curves. This build a six-

dimensional feature vector x to represent a tibiofemoral joint $x=(AAA, CPA, TPA, CA, MJSW, LJSW)$ for further analysis. The intersection between lower and upper condylar spline curves has been used to measure Joint space width (JSW) along y-axis:

$$Y_{common} = Y_{lower} \cap Y_{upper} \quad (9)$$

Intersection list of y-coordinate is used to search (x, y) points on the lower and the upper Condylar curve. Once the corresponding list of (x', y') pairs has been found, JSW measurement simply become the matter of finding the vertical distance between these pairs as shown in Equation (10) and Figure 14. The more detailed visualization and results can be read from Figure 15.

$$JSW = Y'_{lower} - Y'_{upper} \quad (10)$$

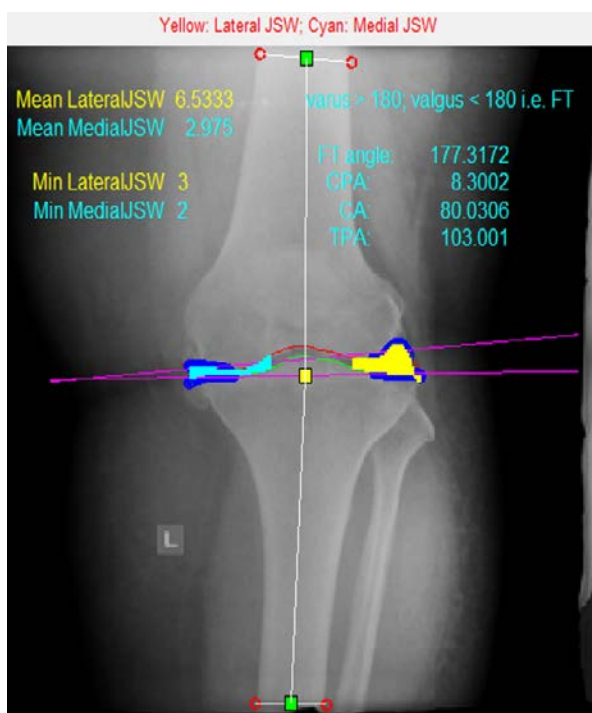


Figure 15: Results of Geometric Analysis

Table I: Statistical analysis.

NO	Quantified Results		
	Parameter	mean	std
1	Mean/Min Median JSW	3.6400 / 2	1.5
2	Mean/Min Median JSW	2.8393/2	2.0
3	Anatomical Axis Angle (AAA)	175.1981	3.3407
4	Condylar Angle (CA)	92.7556	17.0083
5	Tibial Plateau Angle (TPA)	86.6046	11.3131
6	Condylar Plateau Angel (CPA)	6.2177	4.4069

Table I shows the results computer over 40 osteoarthritis patients showing all six mentioned knee parameters. Condylar angle seems to have maximum standard deviation showing some serious improvements needed.

6. CONCLUSION AND FUTURE WORK

Geometric Analysis of Knee Anteroposterior (AP) radiograph has been successfully done to quantify six important knee parameters as shown in Table I. Geometric analysis is accompanied with interesting linear algebra constructs to be used in computer-aided software for automation and treatment planning. All the work has been implemented on MATLAB® and the complete software can be downloaded from the authors' website. Future work comprises validation and improvement of discussed techniques from medical experts especially orthopedic surgeons. Another future dimension is an extension of 2D analysis into 3D analysis for 3D modeling of bone and joints.

7. ACKNOWLEDGMENT

We are thankful to ESSA LABORATORY, KARACHI, PAKISTAN for providing data for academic and research purpose.

8. REFERENCES

- Aguado, & Alberto. (2018). *U.S. Patent No. 10062197, 15/421852*. Washington, DC: U.S. Patent and Trademark Office. Animating a virtual object in a virtual world
- Alnouri, M., Saei, J. A., Younis, M., Bouri, F., Habash, M. A., Shah, M. H., & Dosari, M. A. (2015). Comparison of Edge Detection Algorithms for Automated Radiographic Measurement of the Carrying Angle. *Journal of Biomedical Engineering and Medical Imaging*,2(6). doi:10.14738/jbemi.26.1753
- Belvedere, C., Siegler, S., Fortunato, A., Caravaggi, P., Liverani, E., Durante, S., Leardini, A. (2018). A New Comprehensive Procedure For Custom-Made Total Ankle Replacements: Medical Imaging, Joint Modeling, Prosthesis Design, And 3D Printing. *Journal of Orthopaedic Research*. doi:10.1002/jor.24198
- Burleson, J., & Dipaola, C. (2019). 3D Printing in Spine Surgery. *3D Printing in Orthopaedic Surgery*,105-122. doi:10.1016/b978-0-323-58118-9.00010-5
- Colebatch, A. N., Hart, D. J., Zhai, G., Williams, F., Spector, T. D., & Arden, N. K. (2009). Effective measurement of knee alignment using AP knee radiographs. *The Knee*,16(1), 42-45. doi:10.1016/j.knee.2008.07.007
- Ghorbel, E., Boutteau, R., Boonaert, J., Savatier, X., & Lecoeuche, S. (2018). Kinematic Spline Curves: A temporal invariant descriptor for fast action recognition. *Image and Vision Computing*,77, 60-71. doi:10.1016/j.imavis.2018.06.004
- Gonzalez, R. C., & Woods, R. E. (2008). *Digital image processing*. New Jersey: Parson.
- Goulston, L., Sanchez-Santos, M., Dangelo, S., Leyland, K., Hart, D., Spector, T., . . . Arden, N. (2016). A comparison of radiographic anatomic axis knee alignment measurements and cross-sectional associations with knee osteoarthritis. *Osteoarthritis and Cartilage*,24(4), 612-622. doi:10.1016/j.joca.2015.11.009
- Harvey, W. F., Niu, J., Zhang, Y., Mccree, P. I., Felson, D. T., Nevitt, M., . . . Hunter, D. J. (2008). Knee alignment differences between Chinese and Caucasian subjects without osteoarthritis. *Annals of the Rheumatic Diseases*,67(11), 1524-1528. doi:10.1136/ard.2007.074294
- Harvey, W. F., & Hundter, D. J. (2007). *Knee alignment and Incident Osteoarthritis*(Rep.). Boston University Medical Cneter.
- Imhauser, C., & Schafer, K. (2019). *U.S. Patent No. US010198968B2*. Washington, DC: U.S. Patent and Trademark Office.
- Method for Creating a Computer Model of a joint for Treatment Planning
- Oka, H., Yoshimura, N., Muraki, S., Mabuchi, A., Nakamura, K., & Kawaguchi, H. (2007). 331 Fully Automatic Quantification Of Knee Osteoarthritis Severity On Standard Radiographs By A Novel Computer Assisted System. *Osteoarthritis and Cartilage*,15. doi:10.1016/s1063-4584(07)61962-1
- Okamoto, S., Mizu-Uchi, H., Okazaki, K., Hamai, S., Tashiro, Y., Nakahara, H., & Iwamoto, Y. (2014). Two-dimensional planning can result in internal rotation of the femoral component in total knee arthroplasty. *Knee Surgery, Sports Traumatology, Arthroscopy*,24(1), 229-235. doi:10.1007/s00167-014-3370-1

S., H. J., & M., K. J. (2007). *Computer Graphics Using OpenGL*. Upper Saddle River NJ: Prentice Hall.

Tariq, H., & Burney, S. M. (2012). Contour Extraction of Femur and Tibia Condyles on Plain Anteroposterior (AP) Radiograph. *International Journal of Computer Applications*, 52(15), 26-30. doi:10.5120/8278-1893

The MathWorks, Inc. (n.d.). MATLAB Image Processing and Statistics Toolbox (Version 2014a) [Computer software].

Vitković, N., Mladenović, S., Trifunović, M., Zdravković, M., Manić, M., Trajanović, M., . . . Mitić, J. (2018). Software Framework for the Creation and Application of Personalized Bone and Plate Implant Geometrical Models. *Journal of Healthcare Engineering*, 2018, 1-11. doi:10.1155/2018/6025935.



Dr. Humera Tariq is an Assistant Professor at Department of Computer Science, University of Karachi, Pakistan. She received her B.Eng.(Electrical Engineering) from NED University of Engineering and Technology and Ph.D. (Computer Science) from University of Karachi in 2015. Dr. Humera Tariq's research interest includes image processing, biomedical imaging, Modeling, Simulation, and Machine Learning.



Syed Faraz is a Graduate Research Assistant at Universiti Teknologi PETRONAS, Malaysia. He earned his Bachelor of Science (BS) in Computer and Information Sciences and Support Services from University of Karachi, Pakistan. His interests involve mathematical modeling for intelligent systems.



Asia Samreen is a Senior Assistant Professor at Department of Computer Science, Bahria University, Karachi Campus, Pakistan. Asia Samreen obtained M.Sc. degree in Applied Mathematics from University of Karachi, and an MS degree in Computer Science from PAF-KIET, Karachi, Pakistan. Asia Samreen's researches are Trust Management based on Behavior and Sentiment Analysis for Textual data, Modeling Graph-based Path evaluation, Big Data evaluation for various fields like Health and Opinion Mining.



Dr. Usman Amjad received BS. and Ph.D. in Computer Science from University of Karachi. His research interests include soft computing, machine learning, artificial intelligence, and programming languages. He was the recipient of the HEC Indigenous 5000 scholarship in 2013. Currently, he is working as an AI solution architect at Datics.ai Solutions.

Trademarks Disclaimer: All products names including trademarks™ or registered® trademarks mentioned in this article are the property of their respective owners, using for identification purposes only. Use of them does not imply any endorsement or affiliation.